Water Air Soil Pollut (2009) 203:155–168
DOI 10.1007/s11270-009-9999-6

Nanoparticulate Zeolitic Tuff for Immobilizing Heavy Metals in Soil: Preparation and Characterization

Ayoup M. Ghrair · Joachim Ingwersen · Thilo Streck

Received: 1 August 2008 / Accepted: 26 January 2009 / Published online: 13 February 2009

Abstract Nanoparticles derived from natural materials are promising compounds in the field of environmental remediation. The present study produces and characterizes Na-zeolitic tuff in the nanorange, stabilizes the nanotuff in suspension, and investigates the effect of Na-zeolitic nanotuff on sorption of Cd. Breakdown of raw zeolitic tuff with a mean particle size of 109 μm to the nanorange was achieved by attrition milling. In the first stage of grinding, a mixture of Al-oxide beads of 1 to 2.6 mm diameter was used. The milling process lasted 4 h. In the second stage, the dried powder was milled again using a mixture of a fine zirconia beads (0.1 mm) and Al-oxide beads (1.0 mm). The powder was treated with 1 M NaCl solution. Finally, the powder was sonicated in water. After this procedure, the mean and median particle diameters were 47.6 and 41.8 nm, respectively. The nanoparticulate zeolitic tuff had a surface area of 82 m^2 g^{-1}. The estimated zero charge point of the nanoparticle suspension was 3.2. The surface zeta potential was pH dependent. The Na-zeolitic nanotuff increased Cd sorption by a factor of up to 3 compared to the raw zeolitic tuff. Our results indicate that zeolitic nanoparticles can be produced by grinding using a mixture of fine beads in an attrition mill and that this procedure increases their metal immobilizing potential.

Keywords Nanoparticles · Zeolitic nanotuff · Surface area · Attrition mill · Heavy metals · Sorption · Zeta potential

A. M. Ghrair (✉) · J. Ingwersen · T. Streck
Biogeophysics Section,
Institute of Soil Science and Land Evaluation,
University of Hohenheim,
Emil-Wolff-Str. 27,
70593 Stuttgart, Germany
e-mail: ghrair@uni-hohenheim.de

1 Introduction

Heavy metal contamination of soil is a key concern because of its toxicity, which threatens human life and the environment (Bhogal et al. 2003; Carmichael 1994; Purves 1985). Cadmium (Cd) is of particular interest because it is one of the most bioavailable and mobile heavy metals in soil and the environment. Cadmium is a highly toxic element that is not known to be essential for any type of organism (McBirde 1994). Cd is easily absorbed by roots and transported to shoots. It is then uniformly distributed in plant organs (Sekara et al. 2005). Uptake of Cd by plants depends on several plant and soil factors such as solution-phase concentration, pH, and organic carbon content. Moreover, the environmental conditions (temperature and saturation deficit) may play an important role in controlling Cd uptake (Ingwersen and Streck 2005). Anthropogenic contamination of soils by heavy metals (Cd, Pb, and Zn) occurs from many sources such as mining, atmospheric deposition

from smelting operations, application of sludge, and mineral fertilizers and pesticides (Alloway 1995).

For on-site remediation of heavy-metal-contaminated sites, several soil amendments (among others, zeolitic tuff) have been tested and proposed during the last decades. Zeolitic tuff is a volcanoclastic deposit that contains large amounts of zeolites, reflecting the transformation of magmatic products such as volcanic glass and primary aluminum silicate minerals (Hay and Sheppard 2001). Zeolites are secondary minerals that can be defined as crystalline hydrated aluminosilicates of alkali and alkaline earth cations having an infinite three-dimensional framework (Mumpton 1977).

Natural zeolite minerals have been evaluated as sequestering agents for environmental cleanups and for immobilizing heavy metals in moderately polluted soils (Querol et al. 2006; Knox et al. 2003; Tsitsishvili et al. 1992). Zeolites have been used for a long time in Japan to improve soil quality (Oste et al. 2002). They are added to the soil to control soil pH and nitrogen retention. In wastewater treatment, natural zeolites are used to remove ammonium ions and heavy metals (Singh and Oste 2001; Zamzow et al. 1990) and in the amendment of sewage sludge (Sprynskyy et al. 2007; Nissen et al. 2000). The remediation of soil contaminated by lead and/or cadmium by applying zeolite significantly reduced the solubility of these two heavy metals in the soil (Garau et al. 2007; Fenn et al. 2006).

Kalantari et al. (2006) showed that applying 500 kg ha^{-1} zeolite increased the growth and yield of rice growing in contaminated soils and that the level of plant-available cadmium was reduced by half. The addition of zeolite reduced the Cd content of the rice grain by up to 67% compared to the control. However, the use of zeolites does not always decrease metal availability (Madrid et al. 2008). Similarly, Weber et al. (1984) investigated the effect of natural zeolite amendment on heavy metal uptake by sorghum from an arable soil. They reported no reduction of heavy metal uptake even at an application rate of approximately 6.5% by weight. In addition, other studies showed that applying zeolite only minimally affected the plant availability of metals (Chlopecka and Adriano, 1997, 1996; Baydina 1996).

A factor that limits the use of zeolitic tuff is the high application rate needed to effectively immobilize heavy metals. Zorpas et al. (2003) used an application rate of 25% by weight to obtain significant effects. Brannvall (2006) reported that adding 20% zeolite to polluted sandy soil immobilized 29% Cu, 56% Pb, and 54% Zn.

One of the limiting properties of natural zeolite is its relatively small surface area compared to nanomaterial. Decker et al. (2003) reported that the BET specific surface area of zeolitic tuff was between 7.8 and 12.3 $m^2\ g^{-1}$. B.E.T. (or BET) stands for Brunauer, Emmett, and Teller, the three scientists who optimized the theory for measuring surface area (Brunauer et al. 1938). In contrast, the BET specific surface area of nanoparticles is 50–100 $m^2\ g^{-1}$ (which is considered an intermediate surface area; Kockrick et al. 2008).

Pretreating zeolite with NaCl may significantly increase sorption of pollutants. Athanasiadis and Helmreich (2005) treated clinoptilolite with 1 M NaCl solution at room temperature over a 24-h period. Afterward, the clinoptilolite was washed with ultrapure water and ultrasonicated several times, and then the sample was dried. This pretreatment replaced all exchangeable cations with Na, which is more easily exchangeable than bivalent cations such as Ca or Mg (Cmielewska and Lesny 1995; Bremmer and Schultze 1995).

The starting point of our study was that nanoscale zeolite particles should be a promising candidate for heavy metal immobilization because they provide a large external surface area and can also be easily modified to effectively bind metals species. Nanoparticles provide cost-effective solutions to environmental cleanup problems (Zhang et al. 2004; Zhang 2003).

Nanoparticles are defined as particles with an average characteristic dimension <100 nm (Dutta et al. 2000). Nanoparticles are seen as important auxiliary materials for soil remediation because of their large surface area and other beneficial physical properties. These include magnetic properties, optical properties (e.g., transparency) along with thermal properties and chemical properties such as reactivity (Perez et al. 2004). Nanoparticles can be produced following a bottom-up process, for example synthesis of nanoparticles from solutions, or by a top-down approach in which nanoparticles are produced, e.g., by mechanical attrition (De Castro and Mitchell 2003).

Mechanical milling is widely used in the mineral-processing industry. Here, a powder is subjected to grinding under high-energy compressive impact forces (Zhang et al. 2003). Different types of ball mills—attrition mills, planetary mills, tumber mills,

shaker mills, and vibrator mills—have been manufactured for various purposes. In mechanical attrition, the size of the bulk material is reduced by milling. This is a simple technique with low-cost equipment. Nonetheless, particles produced by this method usually have a broad size distribution, and contamination from the milling machinery is often a problem (Tjong and Chen 2004; Edelstein and Cammarata 1996, Ichinose et al. 1992).

An attrition ball mill (attritor) consists of a rotating vertical drum with a series of impellers which move inside a grinding tank (Kuhn 1984). Attritors are mills in which large quantities of powder (0.5 to 40 kg) can be milled at a time. The grinding tanks are available in stainless steel or stainless steel coated with alumina, silicon carbide, silicon nitride, zirconia, rubber, or polyurethane. Different balls and beads such as glass, flint stones, stealite ceramic, mullite, silicon carbide, silicon nitride, silicon, alumina, zirconium silicate, zirconia, stainless steel, carbon steel, chrome steel, and tungsten carbide are available. Operation of an attritor is simple: The powder to be milled is placed in a container with the balls, and the mixture is then agitated and rotated at a high speed by a shaft with arms. This causes the milling media to exert both shearing and impact forces on the material (De Castro and Mitchell 2003).

Historically, attrition milling was developed for producing metal powders for the purpose of alloying. It was first developed by John Benjamin at the International Nickel company (Kimura et al. 1999). In recent years, this technique has been used to produce a wide range of materials including metastable structures such as amorphous (Koch et al. 1983) and quasicrystalline materials (Eckert et al. 1989). The milling process of material particles to powder size causes attrition between balls, between the balls and the container wall, between the balls and the agitator shaft and the impellers (De Castro and Mitchell 2003). Studies on the production of nanoparticles by mechanical attrition have been reviewed by several researchers such as Koch (1993), Siegel (1991), and Gessinger (1984).

Here, we report for the first time on the preparation of Na-zeolitic tuff in the nanorange by mechanical attrition milling. The objectives of our study were (1) to produce and characterize Na-zeolitic tuff in the nanorange, (2) to stabilize the zeolitic tuff nanoparticle in suspension, and (3) to quantify the extent to which sorption of Cd to zeolitic tuff can be enhanced by converting the raw material to the nanosize.

2 Materials and Methods

2.1 Raw Zeolitic Tuff

Zeolitic tuff was collected from Tell Rimah volcano, northeast of Jordan. The sample was crushed and sieved. The mean particle size was 109 μm (median 119 μm). The total cation exchange capacity (CEC) was 93.4 $cmol_c\ kg^{-1}$. The zeolitic tuff was strongly alkaline (pH 8.8). Exchangeable cations were 6.61% Ca, 4.55% Mg, 1.67% K, and 0.30% Na (by weight).

2.2 Preexperiments

In preexperiments, different mills (planetary ball and attrition ball mill), bead materials (Al-oxide beads and zirconium oxide), bead sizes (from 15 to 0.1 mm), and grinding times (from 0.5 to 20 h) were tested.

2.2.1 Planetary Ball Milling

A planetary ball mill PM 1000 (Retsch GmbH, Haan, Germany) was employed. The designation refers to the rotating support disk, with each jar rotating around its own axis. The rotation speed was 210 rpm. The diameter of the tested zirconium dioxide balls was 15 mm. The ball-to-powder weight ratio was 16. Grinding times ranged between 2 and 20 h without change in the number or diameter of balls.

2.2.2 Attrition Milling

A laboratory-sized PE/PR attrition mill (Attritor, Siemens, Germany) was used. The mill had a chamber and a vertical rotating central shaft with horizontal arms (impellers). The mill chamber was filled with 1.6–2.6 or 1 mm beads of aluminum oxide (Krahn Chemie GmbH, Hamburg, Germany). The weight ratio of beads-to-zeolitic tuff powder was 24. The rotation rate was set to 1,300 rpm. In all cases, ethanol was used as solvent. The milling process involved stirring by the agitator and the impellers. The impellers energize the ball charge. The grinding vessel was jacketed for cooling (Bilgili et al. 2004; De Castro and Mitchell 2003).

2.3 Preparation of Na-Zeolitic Nanotuff

The Na-zeolitic tuff nanoparticles were prepared using the following method: 50 g of raw zeolitic tuff was added to 1,200 g of a mixture of Al-oxide beads (1 and 1.6-2.6 mm diameter, unit weight ratio, KRAHN Chemie GmbH, Hamburg, Germany). The ratio of beads to powder was adjusted to 24 by weight. In the first stage, the zeolitic tuff was milled for 4 h. After that, the milling beads were separated from the suspension with a sieve chain and subsequently dried using a vacuum evaporator. The dry powders were obtained after 15 h of drying at 60°C in a drying oven. In the second stage, the dried powders were milled again for 4 h using 1,600 g of a mixture of 0.1 mm zirconium dioxide beads (YTZ, Tosoh, Co., Japan) and 1.0 mm aluminum oxide beads (KRAHN Chemie GmbH, Hamburg, Germany) in a weight ratio of 2:1. In this stage, the beads to powder weight ratio was 32:1. The suspension was separated from the milling media as described above. Ethanol was separated from the sample in a vacuum evaporator, enabling reuse. The powders were dried in an oven at 60°C over night. After drying, the powders were passed through a 20-μm sieve. Subsequently, each powder was treated with 1 M NaCl solution over a period of 24 h. Finally, the powders were washed with ethanol and sonicated at 100% amplitude and one cycle for 20 min using ultrasonic processors (UP 200S, Germany). To avoid a temperature increase during the sonication process, an ice coat was used.

2.4 Characterization of Zeolitic Tuff Nanoparticles

Size and shape are important properties of nanoparticles. The size distribution of zeolitic tuff nanoparticles was investigated under transmission electron microscopy (TEM). TEM studies were performed using a JEOL100CX II transmission electron microscope (JEOL, Tokyo, Japan) operating at 200 kV and a magnification of ×200,000. For TEM observation, nanoparticles were dispersed on a copper grid. The TEM images were analyzed using the software Image Tool for Windows, Version 3 (The University of Health Science Centre at San Antonio, Texas, USA). A laser diffractometer (Malvern Mastersizer 2000, Malvern Instruments Ltd., UK) was used to measure the agglomerate size distribution. The surface charge (Q) of nanoparticles was characterized by a zeta potential (ζ) measurement. Zeta potential is a measure of the electrostatic potential generated by accumulation of ions that are organized into an electrical double layer at the surface of a particle (Sposito 1984). The zeta potential determines the colloidal stability (Fernandez-Nieves and de las Nieves 1999), as given in the equation:

$$Q = 4\pi\varepsilon\varepsilon_0\zeta\, r(1 + \kappa r) \quad (1)$$

where ε is the relative dielectric constant of medium, ε_0 is the dielectric constant of vacuum, and κr is the electrokinetic radius. The zeta potential was determined by an electroacoustic method using an acoustic and electroacoustic spectrometer (DT-1200, Dispersion Technology Ltd., USA). This instrument was also used to measure the particle size distribution. X-ray powder diffraction patterns were recorded using Cu Kα radiation source on a Scintag X1 powder diffractometer (D-500, Siemens AG, Germany). An ultrasonic processor (UP 200S, Germany) was used for dispersing nanoparticles. The chemical composition of the nanoparticles powder and raw zeolitic tuff was determined by X-ray fluorescence analysis measurements using a sequential X-ray spectrometer (SRS 200, Siemens AG, Germany).

2.5 Sorption Experiment in Aqueous System

Sorption experiments were carried out by adding 0.25 g of nanoparticles to 25 ml 0.01 M $Ca(NO_3)_2$ solution containing Cd at five different concentrations (0.2, 0.5, 1.0, 2.0, or 5.0 mg/l). The samples were shaken for 48 h on a horizontal shaker at 180 rpm and at room temperature (20±2°C). Afterward, the samples were centrifuged at 20,000×g for 30 min (Sorvall Superspeed Fixed-Angle Rotors, Kendro, USA). A 10-ml aliquot of the supernatant was removed and stored in a plastic tube at 4°C. Cd solution phase concentrations were determined by flameless atomic absorption spectrometry (SpectrAA-800, Varian Deutschland GmbH, Germany). Sorbed phase concentrations were calculated from the mass balance. All sorption experiments were conducted using 50 ml polypropylene tubes (Kendro Laboratory Products GmbH, Germany).

After converting measured solution and sorbed phase concentrations to logarithms, the log-transformed

Freundlich equation was fitted to the measured data (Streck et al. 1995):

$$\log S = m \log C + \log k. \quad (2)$$

Here, S (mg kg^{-1}) is the sorbed phase concentration, C (mg L^{-1}) is the concentration of dissolved chemical, k stands for the Freundlich coefficient (mg^{1-m} L^{m} kg^{-1}), and m denotes the Freundlich exponent (≤1).

3 Results

In the grinding process, bead size was the key factor for nanopreparation (Fig. 1). Using 15-mm-diameter Zr-dioxide beads, the mean particle size of raw zeolitic tuff after 4 h of grinding was reduced from 109 μm to a powder with a mean particle size of 3.9 μm. Prolonging grinding to 20 h further reduced the mean particle size to 2.1 μm. Nevertheless, the nanoscale range (<100 nm) was not achieved. Using smaller Al-oxide beads (1.6–2.6 mm diameter) yielded a mean particle size of 1.3 μm after 4 h of continuous grinding. The 1-mm-diameter Al-oxide beads reduced the mean particle size to 1.3 and 1.1 μm after 2 and 6 h, respectively. Zr-dioxide fine beads with a mean diameter of 0.1 mm were unable to grind the zeolitic tuff at all. This can be attributed to the use of a feed particle size whose diameter is larger than the grinding media.

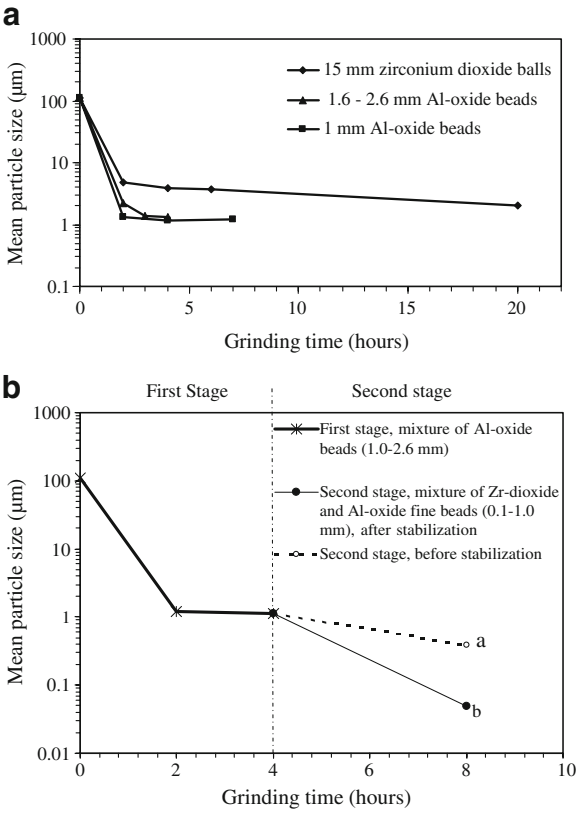

Fig. 1 **a** Mean particle size of zeolitic tuff as a function of grinding time using different grinding material. **b** Grinding progress in the optimized two-stage grinding scheme. Point *a* represents the mean agglomerates size before stabilization, while point *b* represents the mean (single) particle size of the zeolitic nanotuff after stabilization in suspension. Results are means of three replicates

For optimizing and speeding up the grinding procedure, a two-stage grinding process was developed. In the first stage, a mixture of Al-oxide beads (1–2.6 mm) tended to achieve faster milling. Two hours of grinding were sufficient to obtain a particle mean size of 1.2 μm. At the end of the first stage (4 h), the mean particle size was 1.1 μm. In the second stage, a mixture of Zr-dioxide (0.1 mm diameter) and Al-oxide beads (1 mm diameter) were used. The particles' size in the powder was transferred from the micron range to the nanorange. After 8 h of grinding, the nanoparticles tended to form agglomerates (385 nm diameter; Fig. 1, point a). For particle stabilization, the powder was washed with 1 M NaCl and sonicated. At the end of the second stage, the mean particle size of the nanoparticles was 49 nm (Fig. 1, point b). The size was the real particle size, as confirmed by TEM (Fig. 2). The produced nanoparticles had a surface area of 81.9 m^2 g^{-1} and a CEC of 154 $cmol_c$ kg^{-1}.

Attrition milling of raw zeolitic tuff with a mixture of fine Zr-dioxide and Al-oxide beads, during the second stage of grinding, produced submicron-size agglomerates composed of nanosize particles. Figure 2a shows the two types of nanoparticles (single and agglomerated) obtained. TEM imaging showed that the shape of larger nanoparticles tended to be irregularly with smooth edges and wavy grain boundary. The smaller particles were more spherical. The electron diffraction patterns confirmed that the zeolitic tuff nanoparticles were still in the nanocrystalline phase (Fig. 2b). The electron diffraction pattern demonstrated that more than one crystal was overlapping. Hence, the crystal structure was conserved. TEM imaging of the nanoparticles revealed that the mean particle diameter was

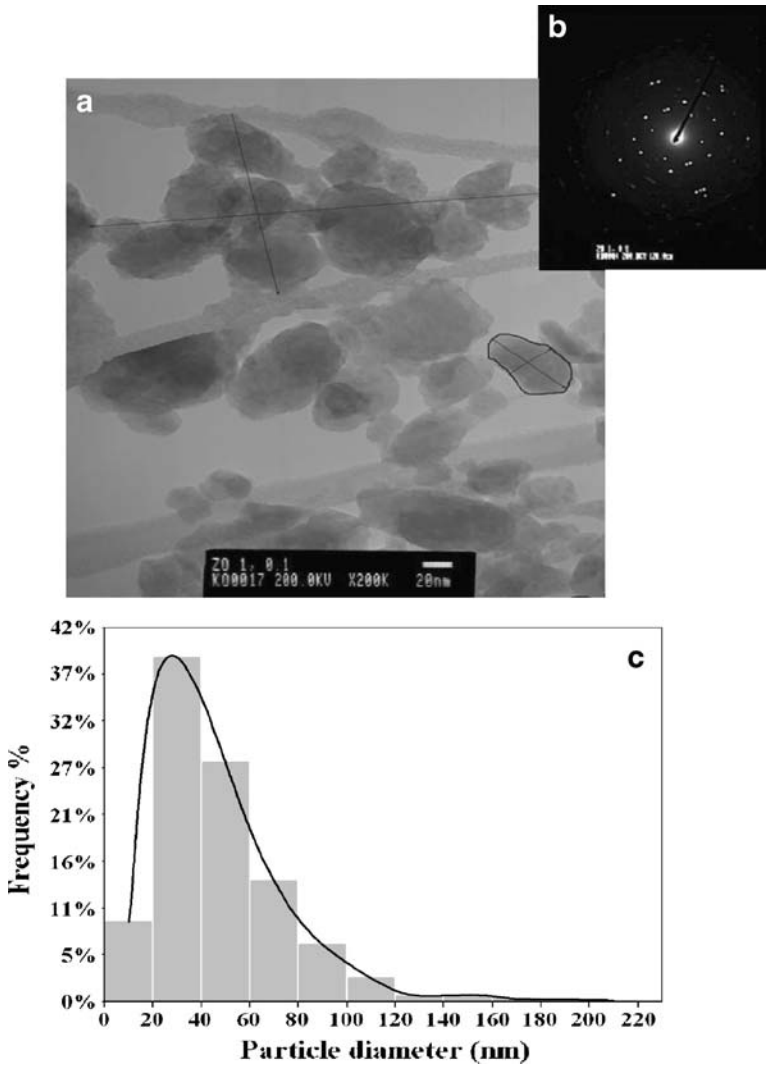

Fig. 2 **a** Zeolitic tuff nanoparticles observed by TEM at 200 kV and ×200,000 magnification. **b** The *inset* shows the electron diffraction pattern. **c** Histogram of the size distribution of zeolitic tuff nanoparticles based on TEM image analysis. Log-normal curve was fitted to the particle size distribution

48 nm (median 42 nm). Based on TEM image analysis, the particle size distribution was log-normal (Fig. 2c).

The laser diffractometry (LD) results (Fig. 3c) confirm those obtained from TEM image analysis (Fig. 2c). Fifty percent of the agglomerate diameters were <359 nm. After stabilizing, the mean particles size was 49 nm (median 48 nm). The particle size distribution was normal before and after stabilization. The difference between the particle size distribution curves, means, and medians obtained using TEM versus LD is attributed to particle shape, morphology, and overlapping. Under the operating conditions of the LD, the particle size distributions were different either because the LD Malvern software is strictly valid for spheres or because the particles adopt preferential orientations in the measurement cell (Gabas et al. 1994). LD considers the measured diameter of any particle as the diameter of a sphere even if the particle is a rod, ellipse, or irregularly shape.

The X-ray diffractogram patterns revealed that the mineral content of zeolitic nanotuff is phillipsite, chabazite, faujasite, calcite, and smectite (Fig. 4). Figure 4 shows that the peak heights (intensity) and width of half heights decrease as grinding time increases and particle size decreases.

The zeta potential measurements show that the surface of the produced zeolitic tuff nanoparticles was negatively charged at pH 3.8–9.3 (Fig. 5). At pH 8.6, the zeta potential of zeolitic nanotuff was −46.3 mV, and the zeta potential of Na-zeolitic nanotuff was −64.6 mV. However, the point at which the graph passes through

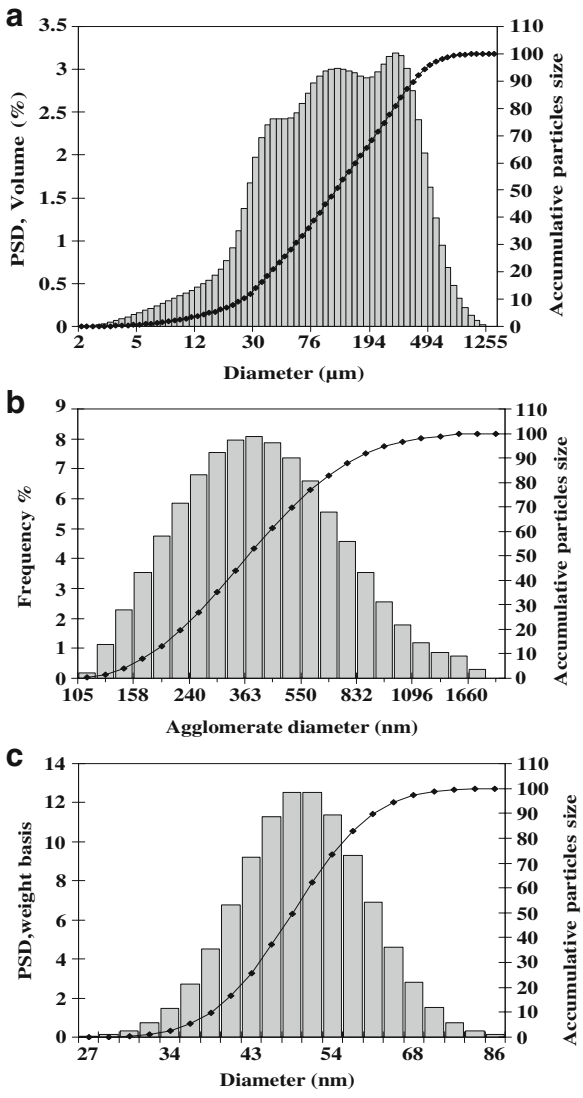

Fig. 3 **a** Particle size distribution of raw zeolitic tuff (feed particle size), **b** particle size distribution of zeolitic tuff agglomerates (median 359 nm), and **c** size distribution of single tuff particles after stabilizing. Size distributions were measured using a laser diffractometer

zero potential was not attainable. For the zeolitic nanotuff, extrapolation of the zeta potential measurements using polynomial third order curves gave an estimated pH of 3.9. In the case of Na-zeolitic nanotuff, the estimation yields pH 3.2. The high negative values of the zeta potential led to a stable nanoparticle suspension, which enables the zeta potentials to be measured over a wide range of pH.

The chemical composition of the raw and modified zeolitic nanotuff is presented in Table 1. The change in the element contents after the Na treatment of the zeolitic nanotuff was due to the change in the exchangeable counter cations. Na partially replaced cations such as Ca, Mg, and K. For example, Na concentration increased by up to 4.1 percentage points from 0.4% to 4.5% by mass. The content of Ca and K decreased by up to 2.9 and 0.8 percentage points, respectively. The Zr-dioxide content was below 0.5% by weight. No increase of the Al-oxide concentration in the final powder was observed when the Al-oxide beads were used.

Sorption Isotherms To investigate the ability of Na-zeolitic nanotuff to immobilize Cd in solution, sorption batch experiments were carried out at various Cd concentrations and pH. The Cd sorption isotherms at pH 4.5, 6.5, and 7.5 are presented in Fig. 6. Figure 6 demonstrates that increasing pH values shift the isotherms toward a higher sorption of Cd. In addition, the double logarithm isotherm was fitted to the linear Freundlich isotherm equation. A positive relation between adsorption and the Cd concentration was found. This is in line with results of many previous studies (Gürel 2006; Voegelin and Kretzschmar 2003; Gao et al. 1997). The isotherm equations reveal that by increasing the pH value from 4.5 to 6.5 or 7.5, the Freundlich coefficient (k) increased 34- or 123-fold, respectively.

Figure 7 compares Cd sorption isotherms of Na-zeolitic nanotuff, Na-raw zeolitic tuff, and raw zeolitic tuff. The slope of the isotherm (m) was similar for Na-zeolitic nanotuff and raw zeolitic tuff (0.69 and 0.68, respectively). The Freundlich coefficient of the Na-zeolitic nanotuff was 5,129 $mg^{1-m}\ L^m\ kg^{-1}$, which is three times higher than that of the raw zeolitic tuff (k=1,585 $mg^{1-m}\ L^m\ kg^{-1}$). Treating raw zeolitic tuff with 1 M NaCl increased the Freundlich coefficient to 2,089 $mg^{1-m}\ L^m\ kg^{-1}$. Yet, transferring the raw zeolitic tuff to the nanorange had a greater effect on sorption than NaCl treatment.

4 Discussion

Grinding raw zeolitic tuff to the nanorange was best achieved by applying a two-stage grinding process using a mixture of large and fine bead sizes. Large beads have more momentum than smaller ones due to their higher mass. Using small beads increases the

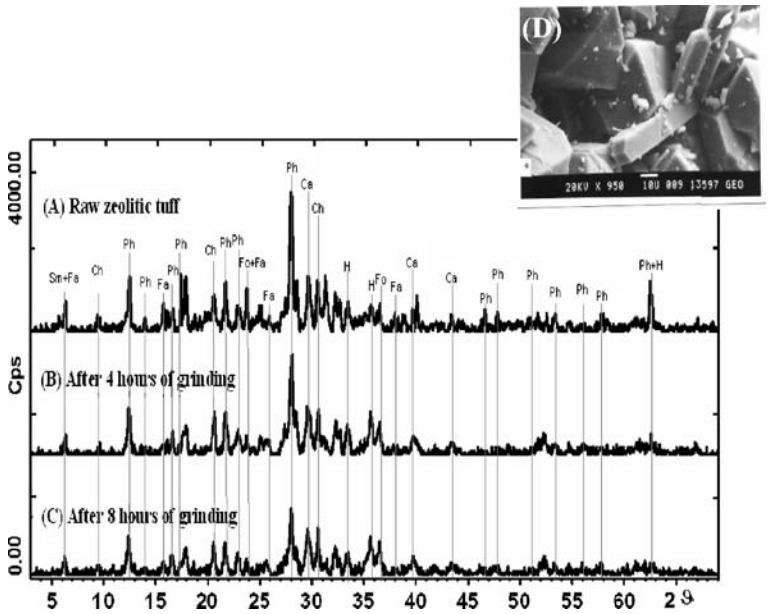

Fig. 4 X-ray diffractometer patterns of zeolitic tuff. *a* Raw zeolitic tuff, *b* raw zeolitic tuff after 4 h of grinding, and *c* raw zeolitic tuff after 8 h of grinding. *Ph* phillipsite, *Sm* smectite, *Ch* chabazite, *Fa* faujasite, *Fo* forsterite, *Ca* calcite, *H* hematite. *d* Simple and penetration twinning crystal growth of raw zeolite minerals. The photograph was taken with a scanning electron microscope

number of collisions because of their higher abundance. It also quickened the milling process. This observation is consistent with previous studies dealing with the optimal bead size for grinding (Bilgili et al. 2004; Way 2004; Jankovic 2003; Zheng et al. 1996). The mean feed particle size for the first stage of grinding was 109 μm, for the second stage about 1 μm (Fig. 1). The ratio between the ultimately selected feeding grain size and ball size was consistent with findings of Way (2004), who reported that for efficient grinding and dispersion, 90% of the feed particle size should have a smaller diameter than 1/10 of the beads' size.

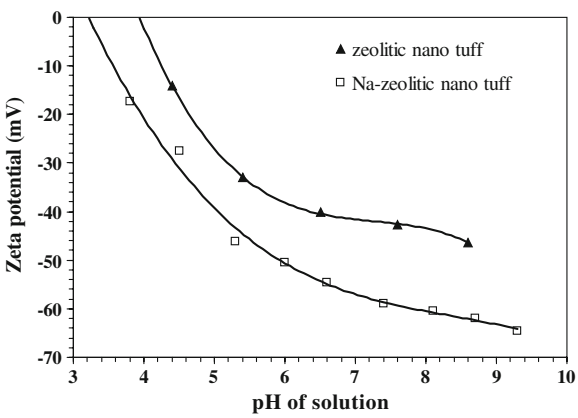

Fig. 5 Zeta potential of zeolitic nanotuff and Na-zeolitic nanotuff. Polynomial third-order curves were fitted to the data points

Compared to other top-down methods for preparing zeolite nanoparticles (e.g., pulsed laser induced fracture or synthesis from colloidal solution), top-down methods present some advantages, such as the low production costs and high yield (Van Heyden et al. 2008; Nichols et al. 2006). Furthermore, the zeolitic tuff is one of the low-cost raw materials that are available to reduce the transfer of heavy metals into the human food chain (Puschenreiter et al. 2005).

The TEM image analysis of the zeolitic nanotuff (Fig. 2a) for obtaining the grain size distribution was time consuming. Particle overlap complicated assigning a contour to each particle. In contrast, in the stabilized suspension, the size distribution of single particles could easily be measured using laser scattering analysis. The mean particle size (48.8 nm) measured by laser scattering was nearly the same as that derived by TEM (47.6 nm). The electron diffraction pattern of the zeolitic nanotuff indicated a disordered arrangement of white spotlights (Fig. 2b). This might be due to the overlapping of the zeolitic tuff nanocrystalline-lattice area. The electron diffraction patterns could appear as white spotlights or circle lights. The white spotlights in the diffraction pattern represent the distribution of atoms within the crystals. Areas with orderly arranged spotlights are termed the lattice area of single crystal (Kimura et al. 1999), while the white circle-lights

Table 1 Chemical composition of the natural and modified zeolitic tuff nanoparticles

Oxide	Oxide content			
	Raw zeolitic tuff (% by weight)	Zeolitic nanotuff (% by weight)	Na-zeolitic nanotuff (% by weight)	±SD[a] (% by weight)
SiO_2	44.82	44.09	44.79	2.13
Al_2O_3	15.64	13.94	14.44	0.89
Fe_2O_3	11.14	13.64	12.28	0.13
Na_2O	0.41	0.40	4.47	0.15
CaO	10.05	8.73	7.18	0.07
MgO	10.20	10.81	9.73	0.20
K_2O	2.18	1.56	1.30	0.15
MnO	2.65	2.40	2.38	0.00
TiO_2	2.32	3.14	2.85	0.04
P_2O_5	0.40	0.34	0.35	0.01
ZrO_2	0.02	0.60	0.49	0.00

[a] Standard deviation of the measurements

represent the amorphous material (Al et al. 2000). Figure 2 illustrates the microstructure of a powder composed of nanocrystalline particles surrounded by very fine amorphous grains. The grain sizes of the zeolitic tuff ranged from 26 to 86 nm (Fig. 3c). Ameyama et al. (1998) and Gleiter (1989) reported that many of the materials milled in mechanical attrition devices were crystalline and had a wavy grain boundary and that the crystallite (grain) size diameter after milling was often between 1 and 10 nm. They

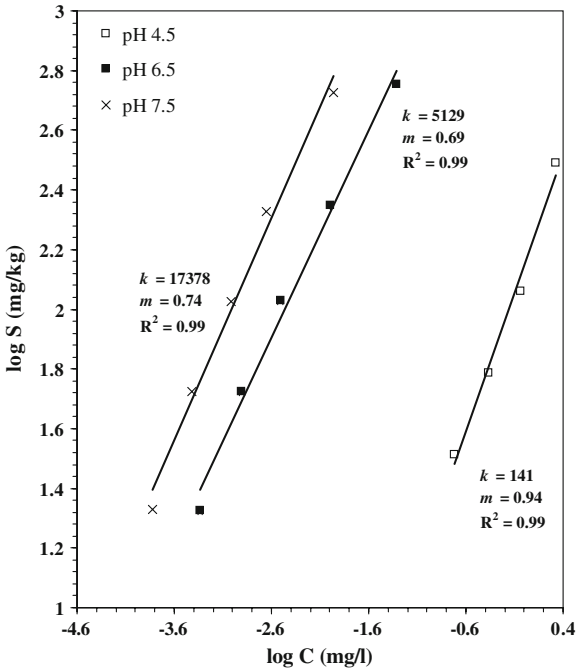

Fig. 6 Freundlich adsorption isotherms of cadmium for Na-zeolitic nanotuff at pH 4.5, 6.5, and 7.5. Each data point was measured in triplicate. The symbols *k* and *m* are the parameters of the Freundlich isotherm log $S=m$ log $C+k$

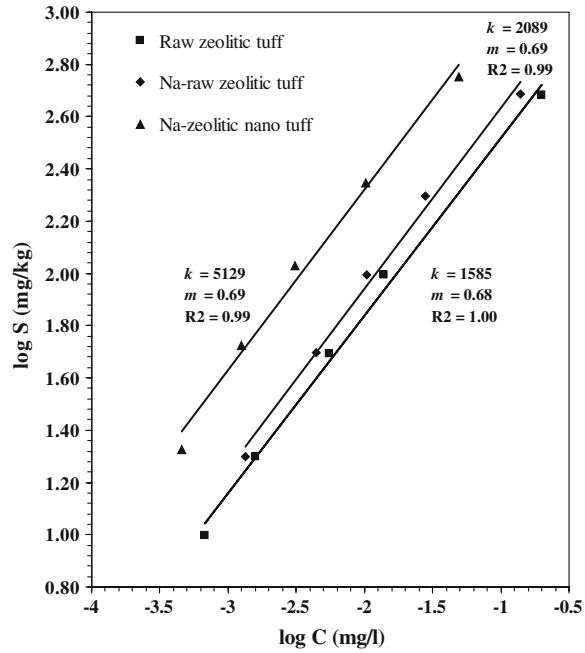

Fig. 7 Freundlich adsorption isotherms of Cd for raw zeolitic tuff, Na-raw zeolitic tuff, and Na-zeolitic nanotuff at pH 6.5. Each data point was measured in triplicate. The symbols *k* and *m* are the parameters of the Freundlich isotherm log $S=m$ log $C+k$

termed such material as nanocrystalline. Other authors (Eckert et al. 1989; Schultz 1988; Koch et al. 1983) have used attrition milling to produce amorphous phase formation.

After milling, traces of ZrO_2 were found in the zeolitic nanopowder (Table 1) as impurities and contamination, which could not be totally avoided in mechanical grinding. The ZrO_2 content in the final powder was not a serious problem. ZrO_2 shows an adsorption potential comparable to some commercially available materials such as iron-based oxides and hydroxides (Hristovski et al. 2008). The ZrO_2 portion of the final nanomaterial is small (<0.5% by weight). Therefore, we may assume that it is negligible in Cd sorption. Nanomaterials in form of milled powders usually contain contamination elements generated during milling (Tellkamp et al. 2001; Eckert et al. 1992) because, during mechanical attrition, collision occurs between the grinding medium and the vessel and between the grinding balls themselves. Consequently, both the grinding medium and vessel deteriorate and abrade. Contamination therefore increases with increasing milling energy and milling time. One method to avoid contamination is to use a grinding medium and vessel of the same composition as the powder being milled (Han et al. 2005; De Castro and Mitchell 2003). Zeolites are hydrous aluminum silicates. Therefore, Al-oxide beads were used at the first stage of grinding. At the second stage of grinding, however, zirconium dioxide beads (0.1 mm) were used because the fine bead size (0.1 mm) was only available as zirconium dioxide. Grinding the raw zeolitic tuff to the nanorange increased the BET surface area by a factor of 10. Among nanoparticles, Na-zeolitic nanotuff has an intermediate surface area (Kockrick et al. 2008).

Zeolitic tuff is a negatively charged volcanic mineral that attracts positively charged compounds and traps them in its cage-like structure. According to the classification scheme of Riddick (1968), the stability of the Na-zeolitic nanoparticles was very good to extreme at pH>8. The suspension stability was acceptable at pH values between 5.0 and 8.0, where the zeta potential ranged from −40 to −60 mV. At pH 3, the particles stuck together in suspension and eventually formed agglomerates. According to Rumpf (1962), the two forces influencing agglomeration of particles in solution are Van der Waals force and the repulsive force. The latter one is strongly depending on ionic strength and zeta potential. The Van der Waals force increases with decreasing grain size (Brar 2000). The point of zero charge (PZC) was not attained because the suspension was not stable at pH<3.8. This observation is in agreement with the estimated point of zero charge of pH 3.2. PZC is the pH value at which the net total particle charge becomes zero. At this pH value, particles do not move in an applied electrical field (electrophoretic mobility measurement; Sposito 1989). At PZC, the suspension is unstable because the Van der Waals force is higher than the repulsive force. The zeta potential strongly influences the ability of water or liquid to carry nanoparticles in suspension. At low pH, zeolitic tuff nanoparticles form large agglomerates and precipitate. In the present work, the agglomeration problem was overcome by sonication after replacing the counter cations with Na. In the presence of monovalent cations, the diffuse layer tends to enlarge, making the suspension more stabile.

The X-ray diffraction patterns indicate that the zeolitic tuff sample contains three types of zeolite minerals: phillipsite, chabazite, and faujasite. The average channel diameter was 0.43 nm for phillipsite, 0.37 nm for chabazite, and 0.74 nm for faujasite (Barrer 1978). This means that the nanocrystalline zeolite (26–86 nm) may still consist of a conservative channel system because crystal size exceeds channel diameter.

Figure 6 shows that by increasing pH, the Cd isotherms shift toward higher Cd sorption. The Freundlich coefficient k is a measure for the sorption strength of a solute (Ingwersen 2001; Springob and Böttcher 1998). The increase of the Freundlich coefficient with increasing pH is attributed to several factors.

First, increasing the pH increases the electrostatic interaction with Cd^{2+}, which increases sorption. Electrostatic interactions are important for the sorption process (Morais et al. 2007). This is confirmed by the zeta potential drop from −17 mV at pH 3.8 to −64 mV at pH 9.3. The effect of pH on Cd adsorption partly reflects changes in the net proton charge on the soil particles. Second, Naidu et al. (1994) found that the type of interaction (inner-sphere or outer-sphere surface complexation) between Cd and solid phase depends on pH. The hydrolysis properties of Cd^{2+} play an important role in the relation between sorption and pH. Surface complexation is influenced by pH,

whereas ion exchange is influenced by ionic strength (Wu et al. 2007; Wang et al. 2005). Choi (2006) reported that, based upon two geochemical models (surface complex modeling and the Langmuir model) of Cd adsorption to the reference materials smectite and vertisol, the basal plane siloxane cavities are apparently the most important sites for Cd complexation at pH<6.5. For the pH-dependent sites, the edge-site aluminol appears to be the dominant functional surface group responsible for Cd adsorption at pH>6.5. The combination of the zeta potential, surface complexation, and surface functional group of the Na-zeolitic nanotuff and the hydrolysis properties of the Cd^{2+} are responsible for the high impact of pH on sorption.

The sorption isotherms presented in the results (Fig. 7) demonstrate that the efficiency of Na-zeolitic nanotuff for immobilizing Cd from solution was up to 3.2 times higher than that of the raw zeolitic tuff and up to 2.5 higher than the Na-raw zeolitic tuff. The increase of Na-zeolitic nanotuff sorption is related to decreasing the grain size of the raw zeolitic tuff to the nanorange and hence to the higher surface area, higher absolute zeta potential, and total CEC. Grinding the raw tuff to the nanorange can expose most of the atoms of a nanoparticle on the surface. Consequently, the surface atoms can bind with other atoms and enhance the adsorption (Liang et al. 2000). Grinding of the raw zeolitic tuff was probably associated with increasing broken edges, corners, and chemical bonds. Thus, the number of free sorption sites may have been increased and the immobilization potential enhanced.

The increase of Cd sorption on Na-zeolitic nanotuff by up to three times compared with the raw tuff is less than the expected. Perhaps the zeolitic channel system was partially clogged or covered with very fine powder during the grinding process (Inglezakis et al. 1999; Carland and Aplan 1995). Another possible explanation could be addition of HNO_3 to the zeolitic nanotuff during the sorption experiment (the pH of zeolitic nanotuff was adjusted by HNO_3); this enabled H^+ to occupy part of the free sorption sites on the nanoparticle surfaces and changed the net proton charge of nanoparticles. Nanotuff needed much more HNO_3 than raw tuff to adjust the pH to 6.5. Zeolite minerals have a high affinity for H protons (He et al. 2008; Laborde-Boutet et al. 2006). Furthermore, nanoparticles might partly have been agglomerated during the sorption experiment. Consequently, the increase of surface area and Cd sorption was less than expected.

5 Conclusions and Outlook

The present study establishes and describes a novel method for producing and stabilizing zeolitic tuff in the nanorange. Attrition milling with a mixture of different beads size was suitable for transforming the raw zeolitic tuff to the nanorange. The results clearly demonstrate that a mixture of fine beads effectively both grinds and disperses the powder particles. The obtained suspension was stable over a wide range of pH. Grinding the natural zeolitic tuff to the nanorange increased its surface area, absolute zeta potential, and cation exchange capacity, thereby enhancing its potential for immobilizing heavy metals. Zeolitic nanotuff can therefore be seen as an important auxiliary material in the field of soil remediation. The sorption batch experiments clearly demonstrate that grinding the raw zeolitic tuff increased Cd sorption much more than treating the raw tuff with 1 M NaCl solution.

In conclusion, zeolitic nanotuff is a potential alternative to traditional soil amendments provided that it can be produced at a reasonable price. Future research is needed to study the metal immobilizing effect of the zeolitic nanotuff in soils differing in pH and texture. Investigations are also needed on the applicability and efficiency of this material for soil remediation purposes under field conditions. Nanoparticles have been criticized to cause health problem (Gatti and Montanari 2008; Seaton 2007). The characteristics of nanoparticles that influence toxicity is included the number, size, surface area, shape, solubility, chemical composition, and chemical reactivity (Marconi 2006). We encourage focusing scientific interest on monitoring nanoparticle transport in soil and groundwater as well as the ecotoxicity of nanoparticles.

Acknowledgments The authors would like to express thanks for the support of Prof. Dr. F. Aldinger and Dr. J. Bill from the Max-Planck Institute for Metal Research (Stuttgart, Germany) during many fruitful discussions and for providing the attrition ball mill and testing the nanoparticle powder. This research was supported by the German Academic Exchange Service (DAAD).

References

Al, T. A., Martin, C. J., & Blowes, D. W. (2000). Carbonate-mineral/water interactions in sulfide-rich mine tailings. *Geochimica et Cosmochimica Acta*, *64*(23), 3933–3948. doi:10.1016/S0016-7037(00)00483-X.

Alloway, B. J. (1995). *Heavy metals in soils* (2nd ed.). London: Chapman and Hall.

Ameyama, K., Hiromitsu, M., & Imai, N. (1998). Room temperature recrystallization and ultra fine grain refinement of an SUS316l stainless steel by high strain powder metallurgy process. *Tetsu-To-Hagane/Journal of the Iron and Steel Institute (Japan)*, *84*(5), 37–42.

Athanasiadis, K., & Helmreich, B. (2005). Influence of chemical conditioning on the ion exchange capacity and on kinetic of zinc uptake by clinoptilolite. *Water Research*, *39*, 1527–1532. doi:10.1016/j.watres.2005.01.024.

Barrer, R. M. (1978). *Zeolite s and clay minerals as sorbents and molecular sieves* (pp. 65–70). London: Academic.

Baydina, N. L. (1996). Inactivation of heavy metals by humus and zeolites in industrially contaminated soils. *Eurasain Soil Science*, *28*, 96–105.

Bhogal, A., Nicholson, F. A., Chambers, B. J., & Shepherd, M. A. (2003). Effects of past sewage sludge additions on heavy metal availability in light textured soils: Implications for crop yields and metal uptakes. *Environmental Pollution*, *121*, 413–423. doi:10.1016/S0269-7491(02)00230-0.

Bilgili, E., Hamey, R., & Scarlett, B. (2004). Production of pigment nanoparticles using a wet stirred mill with polymeric media. *China Particuology*, *2*(3), 93–100. doi:10.1016/S1672-2515(07)60032-3.

Brannvall, E. (2006). An experimental study on the use of natural zeolite for Cu, Pb and Zn immobilization in soil. *Geologija*, *56*, 1–4.

Brar, T. (2000). Novel ways of synthesizing zeolite A. Master thesis, The University of Cincinnati, Kharagpur.

Bremmer, P. R., & Schultze, L. E. (1995). Ability of clinoptilolite rich tuffs to remove metal cations commonly found in acidic drainage. In D. W. Ming & F.A. Mumpton (Eds.), *Natural zeolites'93: Occurrence, properties, use* (pp. 397–403). New York: Brockport.

Brunauer, S., Emmett, P. H., & Teller, E. (1938). Adsorption of gases in multimolecular layers. *Journal of the American Chemical Society*, *60*(2), 309–319. doi:10.1021/ja01269a023.

Carland, R. M., & Aplan, F. F. (1995). Improving the ion exchange capacity and elution of Cu2+ from natural sedimentary zeolites. *Minerals & Metallurgical Processing*, *12*(4), 210–218.

Carmichael, W. (1994). The toxins of cyanobacteria. *Scientific American*, *170*, 78–86.

Chlopecka, A., & Adriano, D. C. (1996). Mimicked in-situ stabilization of metals in a cropped soil: Bioavailability and chemical form of zinc. *Environmental Science & Technology*, *30*, 3294–3303. doi:10.1021/es960072j.

Chlopecka, A., & Adriano, D. C. (1997). Influence of zeolite, apatite and Fe-oxide on Cd and Pb uptake by crops. *The Science of the Total Environment*, *207*, 195–206. doi:10.1016/S0048-9697(97)00268-4.

Choi, J. (2006). Geochemical modeling of cadmium sorption to soil as a function of soil properties. *Chemosphere*, *63*, 1824–1834. doi:10.1016/j.chemosphere.2005.10.035.

Cmielewska, H. E., & Lensy, J. (1995). Study of sorption equilibrium in the systems: water solutions of inorganic ions-clinoptilolite. *Journal of Radioanalytical and Nuclear Chemistry*, *201*, 293–301. doi:10.1007/BF02164048.

De Castro, C. L., & Mitchell, B. S. (2003). Nanoparticles from mechanical attrition. In M. I. Baraton (Ed.), *Synthesis, functionalization and surface treatment of nanoparticles* (pp. 1–15). France: University of Limoges.

Decker, D. L., Papelis, C., Hershey, R. L., Harris, R., & Schmett, G. (2003). Temperature dependence of sorption behavior of lead and cesium metal ions on western Pahute Mesa and Reiner Mesa aquifer rocks. Report, Nevada Site Office National Nuclear Security Administration, U.S. Department of Energy, Las Vegas, Nevada, publication no. 45193.

Dutta, M. K., Pabi, S. K., & Murty, B. S. (2000). Thermal stability of nanocrystalline Ni silicides synthesised by mechanical alloying. *Materials Science and Engineering A*, *284*, 219–225. doi:10.1016/S0921-5093(00)00774-7.

Eckert, J., Schultz, L., & Urban, K. (1989). Formation of quasicrystals by mechanical alloying. *Applied Physics Letters*, *55*(2), 117–119. doi:10.1063/1.102394.

Eckert, J., Holzer, J. C., Krill, I. C. E., & Johnson, W. L. (1992). Structural and thermodynamic properties of nanocrystalline fcc metals prepared by mechanical attrition. *Journal of Materials Research*, *7*(7), 1751–1761. doi:10.1557/JMR.1992.1751.

Edelstein, A. S., & Cammarata, R. C. (1996). *Nanomaterials: Synthesis, properties and applications* (p. 596). Bristol: Institute of Physics.

Fenn, M. E., Perea-Estrada, V. M., De Bauer, L. I., Perez-Suarez, M., Parker, D. R., & Centina-Alcala, V. M. (2006). Nutrient status and plant growth effects of forest soils in the basin of Mexico. *Environmental Pollution*, *140*, 187–199. doi:10.1016/j.envpol.2005.07.017.

Fernandez-Nieves, A., & de las Nieves, F. J. (1999). The role of ζ potential in the colloidal stability of different TiO_2/electrolyte solution interfaces. *Colloids and Surfaces A: Physicochemical and Engineering Aspects*, *148*(3), 231–243. doi:10.1016/S0927-7757(98)00763-8.

Gabas, N., Hiquily, N., & Laguerie, C. (1994). Response of laser diffraction particle sizer to anisometric particles. *Particle and Particle Systems Characterization*, *11*(2), 121–126. doi:10.1002/ppsc.19940110203.

Gao, S., Walker, W. J., Dahlgren, R. A., & Bold, J. (1997). Simultaneous sorption of Cd, Cu, Ni, Zn, Pb, and Cr on soils treated with sewage sludge supernatant. *Water, Air, and Soil Pollution*, *93*(1–4), 331–345. doi:10.1007/BF02404765.

Garau, G., Castaldi, P., Santona, L., Deiana, P., & Melis, P. (2007). Influence of red mud, zeolite and lime on heavy metal immobilization, culturable heterotrophic microbial popula-

tions and enzyme activities in a contaminated soil. *Geoderma*, *142*, 47–57. doi:10.1016/j.geoderma.2007.07.011.

Gatti, A. M., & Montanari, S. (2008). Nanopollution: The invisible fog of future wars. *The Futurist*, *42*(3), 32–34.

Gessinger, G. H. (1984). *Powder metallurgy of superalloys* (1st ed., pp. 213–294). London: Butterworth.

Gleiter, H. (1989). Nanocrystalline materials. *Progress in Materials Science*, *33*(4), 223–315. doi:10.1016/0079-6425(89)90001-7.

Gürel, A. (2006). Adsorption characteristics of heavy metals in soil zones developed on spilite. *Environmental Geology*, *51*(3), 333–340.

Han, B. Q., Lavernia, E. J., & Mohamed, F. A. (2005). Mechanical properties of nanostructured materials. *Reviews on Advanced Materials Science*, *9*(1), 1–16.

Hay, L. R., & Sheppard, A. R. (2001). Occurrence of zeolites in sedimentary rocks: an overview. In reviews in mineralogy and geochemistry, natural zeolites, occurrence, properties, applications. In D. L. Bish & D. W. Ming (Eds.), *Reviews in mineralogy and geochemistry, vol 45* (pp. 217–234). Washington, DC: Mineralogical Society of America.

He, N., Xie, H.-b., & Ding, Y.-h. (2008). Computational study on IM-5 zeolite: What is its preferential location of Al and proton siting? *Microporous and Mesoporous Materials*, *111*(1–3), 551–559.

Hristovski, K. D., Westerhoff, P. K., Crittenden, J. C., & Olson, L. W. (2008). Arsenate removal by nanostructured ZrO2 spheres. *Environmental Science & Technology*, *42*(10), 3786–3790.

Ichinose, N., Ozaki, Y., & Karsu, S. (1992). *Superfine particle technology* (p. 223). London: Springer.

Inglezakis, V. J., Diamandis, N. A., Loizidou, M. D., & Grigoropoulou, H. P. (1999). Effect of pore clogging on kinetics of lead uptake by clinoptilolite. *Journal of Colloid and Interface Science*, *215*, 54–57.

Ingwersen, J. (2001). The environmental fate of cadmium in the soils of the waste water irrigation area of Braunschweig. Ph.D. dissertation, Braunschweig University, 170p.

Ingwersen, J., & Streck, T. (2005). A regional-scale study on the crop uptake of cadmium from sandy soils: measurement and modeling. *Journal of Environmental Quality*, *34*, 1026–1035.

Jankovic, A. (2003). Variables affecting the fine grinding of minerals using stirred mills. *Minerals Engineering*, *16*(4), 337–345.

Kalantari, M. R., Shokrzadeh, M., Ebadi, A. G., Mohammadizadeh, C., Choudhary, M. I., & Atta-ur-Rahman, (2006). Soil pollution by heavy metals and remediation (Mazandaran-Iran). *Journal of Applied Sciences*, *6*(9), 2110–2116.

Kimura, Y., Takaki, S., Suejima, S., Uemori, R., & Tamehiro, H. (1999). Ultra grain refining and decomposition of oxide during super-heavy deformation in oxide dispersion ferritic stainless steel powder. *ISIJ International*, *39*(2), 176–182.

Knox, A. S., Kaplan, D. I., Adriano, D. C., Hinton, T. G., & Wilson, M. D. (2003). Apatite and phillipsite as sequestering agents for metals and radionuclide. *Journal of Environmental Quality*, *32*, 515–525.

Koch, C. C. (1993). The synthesis and structure of nanocrystalline materials produced by mechanical attrition: A rev. *Nanostructured Materials*, *2*(2), 109–129.

Koch, C. C., Cavin, O. B., McKamey, C. G., & Scarbrough, J. O. (1983). Preparation of "amorphous" Ni60Nb40 by mechanical alloying. *Applied Physics Letters*, *43*(11), 1017–1019.

Kockrick, E., Krawiec, P., Petasch, U., Martin, H., Herrmann, M., & Kaskel, S. (2008). Porous CeO_x/SiC nanocomposites prepared from reverse polycarbosilane-based microemulsions. *Chemistry of Materials*, *20*(1), 77–83.

Kuhn, E. (1984). *Powder metallurgy, ASM handbook, vol. 7* (pp. 56–70) Materials Park, OH: ASM International.

Laborde-Boutet, C., Joly, G., Nicolaos, A., Thomas, M., & Magnoux, P. (2006). Selectivity of thiophene/toluene competitive adsorptions onto zeolites. Influence of the alkali metal cation in FAU(Y). *Industrial & Engineering Chemistry Research*, *45*(24), 8111–8116.

Liang, P., Qin, Y., Hu, B., Li, C., Peng, T., & Jiang, Z. (2000). Study of the adsorption behavior of heavy metal ions on nanometer-size titanium dioxide with ICP-AES. *Fresenius' Journal of Analytical Chemistry*, *368*, 638–640.

Madrid, F., Diaz-Barrientos, E., & Florido, M. C. (2008). Inorganic amendments to decrease metal availability in soil of recreational urban areas: limitations to their efficiency and possible drawbacks. *Water, Air and Soil Pollution*, *192*, 117–125.

Marconi, A. (2006). Fine, ultrafine particles and nanoparticles in ambient and work environments: Possible health effects and measure of inhaled exposure [Particelle fini, ultrafini e nanoparticelle in ambiente di vita e di lavoro: Possibili effetti sanitari e misura dell'esposizione inalatoria]. *Giornale Italiano di Medicina del Lavoro ed Ergonomia*, *28*(3), 258–265.

McBirde, M. B. (1994). *Environmental chemistry of soils* (p. 406). Oxford: Oxford University Press.

Morais, W. A., Fernandes, A. L. P., Dantas, T. N. C., Pereira, M. R., & Fonseca, J. L. C. (2007). Sorption studies of a model anionic dye on crosslinked chitosan. *Colloids Surf., A*, *310*(1–3), 20–31.

Mumpton, F. A. (1977). *Mineralogy and geology of natural zeolites, vol. 4* (pp. 1–15). Washington: Mineralogical Society of America.

Naidu, R., Bolan, N. S., Kookana, R. S., & Tiller, K. G. (1994). Ionic-strength and effects on the sorption of cadmium and the surface charge of soils. *European Journal of Soil Science*, *45*, 419–429.

Nichols, W. T., Kodaira, T., Sasaki, Y., Shimizu, Y., Sasaki, T., & Koshizaki, N. (2006). Zeolite LTA nanoparticles prepared by laser-induced fracture of zeolite microcrystals. *Journal of Physical Chemistry, B*, *110*(1), 83–89.

Nissen, L. R., Leppy, N. W., & Edwards, R. (2000). Synthetic zeolites as amendments for sewage sludge-based compost. *Chemosphere*, *41*, 265–269.

Oste, L. A., Lexmond, T. M., & Van Riemsdijk, W. H. (2002). Metal immobilization in soils using synthetic zeolites. *Journal of Environmental Quality*, *31*, 813–821.

Perez, J., Bax, L., & Escolano, C. (2004). Roadmaps at 2015 on nanotechnology application in the sectors of: materials, health and medical systems, energy. Report prepared by Willems &van den Wildenberg.

Purves, D. (1985). *Trace-element contamination of the environment*. Amsterdam: Elsevier.

Puschenreiter, M., Horak, O., Friesl, W., & Hartl, W. (2005). Low-cost agricultural measures to reduce heavy metal transfer into the food chain—a review. *Plant, Soil Environ*, *51*(1), 1–11.

Querol, X., Alastuey, A., Moreno, N., Alvarez-ayuso, E., Garacia-Sanchez, A., Cama, J., Ayora, C., & Simon, M. (2006). Immobilization of heavy metals in polluted soils by the addition of zeolitic material synthesized from coal fly ash. *Chemoshere*, *62*, 171–180.

Riddick, T. (1968). *Control of colloid stability through zeta potential; with a closing chapter on its relationship to cardiovascular disease*. Wynnewood, PA: Livingston. Published for ZETA–METER, INC. 372p.

Rumpf, H. (1962). The strength of granules and agglomerates. In W. Knepper (Ed.), *Agglomeration* (pp. 281–304). New York: Wiley.

Schultz, L. (1988). Formation of amorphous metals by mechanical alloying. *Materials Science and Engineering*, *97*, 15–23.

Seaton, A. (2007). Nanotoxicology: Hazard and risk. PulPaper 2007 Conference: Innovative and sustainable use of forest resources, 1 p

Sekara, A., Poniedzialek, M., Ciura, J., & Jedrszczyk, E. (2005). Cadmium and lead accumulation and distribution in the organs of nine crops: implications for phytoremediation. *Polish Journal of Environmental Studies*, *14*(4), 509–516.

Siegel, R. W. (1991). Cluster-assembled nanoparticles materials. *Annual Review of Material Science*, *21*, 559–578.

Singh, B. R., & Oste, L. (2001). In situ immobilization of metals in contaminated or naturally metal-rich soils. *Environmental Review*, *9*, 81–97.

Sposito, G. (1984). *The surface chemistry of soil, vol. 231* (pp. 78–106). New York: Oxford University Press.

Sposito, G. (1989). *The chemistry of soils*. New York: Oxford University Press.

Springob, G., & Böttcher, J. (1998). Parameterization and regionalization of Cd sorption characteristics of sandy soils. I. Freundlich type parameters. *Zeitschrift fuÉr PflanzenernaÉhrung und Bodenkunde*, *161*, 681–687.

Sprynskyy, M., Kosobucki, T., Kowalkowski, B., & Buszewski, B. (2007). Influence of clinoptilolite rock on chemical speciation of selected heavy metals in sewage sludge. *Journal of Hazardous Materials*, *149*, 310–316.

Streck, T., Poletika, N. N., Jury, W. A., & Farmer, W. J. (1995). Description of simazine transport with rate-limited, two-stage, linear and nonlinear sorption. *Water Resources Research*, *31*(4), 811–822.

Tellkamp, V. L., Melmed, A., & Lavernia, E. J. (2001). Mechanical behavior and microstructure of a thermally stable bulk nanostructured Al alloy. *Metallurgical and Materials Transactions. A, Physical Metallurgy and Materials Science*, *32*(9), 2335–2343.

Tjong, S. C., & Chen, H. (2004). Nanocrystalline materials and coatings. *Materials Science and Engineering R: reports*, *45*(1–2), 88.

Tsitsishvili, G. V., Andorikashvili, T. G., Kirov, G. N., & Filizova, L. D. (1992). *Natural zeolites*. New York: Horwood.

Van Heyden, H., Mintova, S., & Bein, T. (2008). Nanosized SAPO-34 synthesized from colloidal solutions. *Chemistry of Materials*, *20*(9), 2956–2963.

Voegelin, A., & Kretzschmar, R. (2003). Modelling sorption and mobility of cadmium and zinc in soils with scaled exchange coefficients. *European Journal of Soil Science*, *54*(2), 387–400.

Wang, X. K., Chen, C. L., Du, J. Z., Tan, X. L., Xu, D., & Yu, S. M. (2005). Effect of pH and aging time on the kinetic dissociation of ^{243}Am(III) from humic acid coated γ-Al_2O_3: A chelating resin exchange study. *Environmental Science & Technology*, *39*, 7084–7088.

Way, H. W. (2004). Grinding and dispersing nanoparticles. *JCT, Journal of Coatings Technology*, *1*(1), 54–60.

Weber, M. A., Barbarick, K. A., & Westfall, D. G. (1984). Application of clinoptilolite to soil amended with municipal sludge. In W. G. Pond, & F. A. Mumpton (Eds.), *Zeo-agriculture, use of natural zeolite in agriculture and aquaculture* (1st ed., pp. 263–271). Boulder, CO: Westview.

Wu, W., Fan, Q., Xu, J., Niu, Z., & Lu, S. (2007). Sorption–desorption of Th(IV)on attapulgite: effects of pH, ionic strength and temperature. *Applied Radiation and Isotopes*, *65*, 1108–1114.

Zamzow, M. J., Eichbaum, R., Sandgren, K. R., & Shanks, D. E. (1990). Removal of heavy metals and other cations from wastewater using zeolites. *Separation Science and Technology*, *25*, 1555–1569.

Zhang, W. (2003). Nanoscale iron particles for environmental remediation: An overview. *Journal Of Nanoparticle Research*, *5*, 323–332.

Zhang, Y., Yu, X., Wang, X., Shan, W., Yang, P., & Tang, Y. (2004). Zeolite nanoparticles with immobilized metal ions: isolation and MALDI-TOF-MS/MS identification of phosphopeptides. *Chemical Communications*, 2882–2883.

Zheng, J., Harris, C. C., & Somasundaran, P. (1996). A study on grinding and energy input in stirred media mills. *Powder Technology*, *86*(2), 171–178.

Zorpas, A. A., Arapoglou, D., & Panagiotis, K. (2003). Waste paper and clinoptilolite as a bulking material with dewatered anaerobically stabilized primary sewage sludge (DASPSS) for compost production. *Waste Manager*, *23*, 27–35.